Applied Catalysis B: Environmental 176–177 (2015) 472–479

Contents lists available at ScienceDirect

Applied Catalysis B: Environmental

journal homepage: www.elsevier.com/locate/apcatb

Hybrid sol–gel porous nanocomposites as efficient photocatalytic coatings: Insights in the structure/reactivity relationships

D. Gregori[a,b], C. Guillard[a,*], I. Benchenaa[a,c], D. Leonard[c], S. Parola[b]

[a] Institut de Recherches sur la Catalyse et l'Environnement (IRCELYON), UMR 5256, Université de Lyon, UMR CNRS – Université Claude Bernard-Lyon 1, 2 avenue Albert Einstein, 69626 Villeurbanne Cedex, France
[b] Laboratoire de Chimie de L'ENS, UMR 5182, Ecole Normale Supérieure de Lyon, CNRS, Université Claude Bernard-Lyon 1, 46 allée d'Italie, 69364 Lyon Cedex 07, France
[c] Institut des Sciences Analytiques (ISA), UMR 5280, Université de Lyon, UMR CNRS – Université Claude Bernard-Lyon 1 – ENS de Lyon, 5 rue de la Doua, 69100 Villeurbanne, France

ARTICLE INFO

Article history:
Received 22 December 2014
Received in revised form 21 March 2015
Accepted 3 April 2015
Available online 7 April 2015

Keywords:
TiO_2/SiO_2 coating
Photocatalytic activity
UV treatment
Water depollution
Self-cleaning

ABSTRACT

Stability and photocatalytic efficiency of hybrid composite films obtained by efficient dispersion of anatase TiO_2 nanoparticles in various hybrid silica matrices are investigated in order to address the structure/reactivity relationship. The photocatalytic activity is systematically monitored as a function of the chemical composition of the matrix at the molecular level, and thus the final structure of the material. The partial elimination of the organic groups brings by the organosilane precursors under UV exposure was followed by HPLC and by surface analysis (XPS, contact angle). The impact of the alkoxysilane structure on the final structure of the matrix is evaluated. In the same way, the impact of thermal and photonic pretreatments on the coating photocatalytic activity is evaluated using formic acid as model pollutant. Finally, the role of the remaining organic groups in the silica network on the structure modification and on the photocatalytic activity is investigated by varying their nature and ratio. Depolluting and self-cleaning activities of optimized coatings are studied by degrading formic acid and methylene blue in different conditions of pollutant concentration and photon flux. We interestingly show that in all cases, the presence of the organic groups in the matrix induces an increase in the photocatalytic efficiency. Finally, efficient photocatalytic flexible films are prepared and show promising photocatalytic degradation mechanism under low UV excitation, comparable to solar UV irradiation.

1. Introduction

Photocatalytic process is widely developed for self-cleaning, antibacterial and water/air depolluting properties. Indeed the possibility to further use the solar natural energy source, easily accessible, to address depollution problems, energy conversion or catalytic chemical processes, presents an elegant and attractive alternative to commonly used energy consuming technologies. The number of publications in the field has increased exponentially during the last few years [1] due to wide interest in such sustainable technology approach. TiO_2 is the most commonly used photocatalyst due to its high efficiency and large scale commercial availability at reasonable price. On a mechanistic point of view, photocatalysis is initiated by the photogeneration of electron/hole pairs in the semiconductor under excitation by absorption of light with energy equal to or higher than the corresponding band gap. In the particular case of TiO_2 with anatase crystallographic phase, the band gap is E_g = 3.2 eV [2,3,4]. The electrons and holes can become available for redox reactions with electron-donor or acceptor species adsorbed at the semiconductor surface. However, applications remain limited in the case of organic substrates such as textiles, papers and plastics. The main reason is that these substrates are easily damaged under UV irradiation and the induced photocatalytic reactions at the interface cause defects and decomposition leading to coloration, cracks and often heavy degradation [5,6]. Moreover, low cohesion between nanoparticles and substrate usually leads to an important photocatalyst release in environment [7]. These substrates also require low temperature of process to avoid their thermal deterioration. In this context, the sol–gel process operating at low temperature is widely reported for the synthesis of TiO_2 powders [8–11] or coatings [12–14] on such thermosensitive substrates. Most of the time, a protective interface is added between the substrate and the photocatalyst which can also act as an adhesion promoting layer [15–18]. The important drawback

* Corresponding author. Tel.: +33 4 72 44 53 16; fax: +33 4 72 44 53 99.
E-mail address: chantal.guillard@ircelyon.univ-lyon1.fr (C. Guillard).

http://dx.doi.org/10.1016/j.apcatb.2015.04.005
0926-3373/

of such inorganic interface is that it induces coating rigidity. It is shown that flexible coating of silica can be obtained synthesizing hybrid framework containing organic bonds [19,20]. Organic compounds can also be used to generate porosity and improve the coating photocatalytic activity [21–23] but they often require harsh thermal treatment for total removal. Other techniques are proposed in the literature to degrade templating organic compounds at low temperature. Various oxidation agents are employed including ozone [24,25] and hydrogen peroxide [26,27]. UV irradiation is also applied to remove templating agent in mesoporous materials [28,29]. Recent works are also dedicated to cold plasma treatments [30–33]. Within a cold plasma, electrons can be very hot (up to 10^5 K), but the bulk temperature is only slightly higher than room temperature [31].

We propose here to investigate the structure/properties relationship in composite films consisting of commercial TiO_2 nanoparticles dispersed into a porous hybrid silica based binder. The objectives of this study are to compare the efficiency and stability of matrices containing various organic groups, tuning some parameters such as the size or the ratio of the organic pendant groups. UV and thermal pretreatments are optimized to promote the coating stability and activity. The photocatalytic activity of the composite coatings is also determined at different pollutant concentrations and photon fluxes using formic acid and methylene blue as models.

2. Experimental

2.1. Materials preparation

2.1.1. Chemicals

All chemicals are used as received without any further purification. TEOS (tetraethoxysilane), MTEOS (methyltriethoxysilane), VTMOS (vinyltrimethoxysilane) and PTEOS (propyltriethoxysilane) precursors are supplied from ABCR. Absolute ethanol, acetic acid and hydrochloric acid are purchased from Carlo Erba. Citric acid and diethyl ether are provided from Aldrich. Commercial titanium dioxide nanoparticles are supplied from Evonik (Aeroxide P25, anatase/rutile forms with a ratio between 70/30 and 80/20, size between 25 and 35 nm). Formic acid (99% pure) and methylene blue (99% pure) for photocatalytic degradation tests are supplied, respectively, from Across Organics and Aldrich. Milli-Q water (18MΩ) is used for all the syntheses and analyses.

2.1.2. Preparation of the various silica matrices

The hybrid silica sol is prepared using acidic catalysis and condensation of alcoxysilane precursors [20,34,35].

Inorganic silica sol is synthesized through the hydrolysis of 1 mol of TEOS precursor with a solution made of 3 mol of acidic water at pH 2.5 (HCl) and 3 mol of ethanol. Synthesis of silica sols containing methyl or propyl groups consists in the acidic hydrolysis of MTEOS or PTEOS precursors with acidic water at pH 3.8 (HCl). The hydrolysis ratio is [water]/[precursor] = 14. All mixtures are vigorously stirred overnight at room temperature. Silica sol functionalized with vinyl groups is synthesized using the hydrolysis of VTMOS precursors with acidic water (citric acid, 10 g/L). The hydrolysis molar ratio is [water]/[precursor] = 12. This solution is heated overnight at 35 °C under stirring.

The TEOS based sol is conserved without any further modification. For MTEOS and PTEOS sols, the alcohol, generated during the hydrolysis of the precursors, is removed using distillation at 130 °C. For VTMOS sol, alcohol is removed by evaporation under reduced pressure. The sols are extracted from water with ether. The ether phase is washed with water in order to remove the remaining traces of acid. Finally, ether is evaporated under reduced pressure and replaced by ethanol, the final solvent.

All sols are stored at −24 °C. The condensation ratios of the TEOS, MTEOS, PTEOS, and VTMOS sols, calculate from ^{29}Si NMR spectra, are, respectively, 80, 88, 62 and 88%.

2.1.3. Preparation of photocatalytic composite coatings

In order to efficiently disperse the titanium dioxide nanoparticles in the sol, a paste is formed by mixing the titanium dioxide particles with acetic acid. The paste is dispersed in ethanol assisted by sonication for 1 min (ultrasound tip). The final mass ratio in TiO_2/acetic acid/ethanol is 1/0.8/6.4. The silica sol is added to the titanium dioxide dispersion. The quantity of sol introduced is adjusted according to the dried solid residue to obtain a final solution composed of 10% in weight of silica and 10% in weight of TiO_2. The solution is sonicated for 1 min (ultrasound tip) prior to deposition onto silicon wafers. Silicon substrates (9 cm^2) are coated using dip-coating method with a withdrawal rate of 50 mm/min, and dried in the air at 120 °C for 20 h. Image of the deposited coating can be seen in Fig. SI1.

2.1.4. Coatings treatments: temperature and irradiation

The final structure stabilization of the coatings requires further treatment. The influence of two types of treatments is studied, (i) a thermal treatment at 120 °C or 200 °C during either 20 h or 7 days, (ii) a UV treatment in an irradiation chamber (Bio-link, Fisher Scientific, LxPxH = 260 × 330 × 145 mm) consisting of 6 UV lamps operating at a wavelength of 254 nm or 365 nm. The samples are irradiated during different times at a photon flux of 5 mW/cm^2.

2.2. Characterization of the composite coatings

The surface morphology and thickness of coatings are evaluated using scanning electron microscopy (SEM) with a FEI Quanta 250FEG operating at an accelerating voltage of 15 kV. Surface chemical characterizations are performed by X-ray photoelectron spectroscopy (XPS). XPS measurements are carried out using a PHI Quantera SXM instrument (Physical Electronics, Chanhassen, USA) equipped with a 180° hemispherical electron energy analyzer and a monochromatized Al Kα (1486.6 eV) source operated at 15 kV and 4 mA. The analysis spot has a diameter of 200 μm and the detection angle relative to the substrate surface is 45°. The samples are analyzed with dual-beam charge neutralization and the $Ti2p_{3/2}$ component of Ti2p peak is adjusted to 458.8 eV. The atomic concentrations are determined using sensitivity factors provided by the manufacturer. Standard deviations are calculated from measurements performed on two different areas. Amount of TiO_2 into the coatings is determined by ICP-OES (inductively coupled plasma - optical emission spectrometry) using Activa (Jobin Yvon) instrument. Samples are dissolved by acidic attack (H_2SO_4 + HNO_3 + HF) and heat 12 h at 150 °C. The coating hydrophilicity is obtained by contact angle measurements on a Digidrop GBX. Water droplets of 10 μL are automatically deposited. Five measurements in different areas are performed to determine the contact angle value.

2.3. Characterization of the photocatalytic activity of the composite coatings

The photocatalytic experiments are carried out in a in a 90 mL cylindrical Pyrex reactor open to air with an optical window diameter of 4.5 cm. Experiments are performed with an HPK 125 W mercury lamp cooled with a water circulation system avoiding the heating of the solution by removing the IR heating beams. The temperature during the experiment is maintained at about 20 °C. The light spectrum of the lamp is cut off below 300 nm thanks to the use of Pyrex reactor. Total UV radiance intensity received by

the samples is measured by a digital radiometer (VLX-3W, UVItec) equipped with 365 nm ± 5% detector and is of 10 mW/cm^2 for all experiments.

A suspension of 30 mL of formic acid at a concentration of 1086 μmol/L is magnetically stirred in presence of a 9 cm^2 titania-containing substrate in the dark during 30 min to reach the adsorption equilibrium before UV irradiation. Then, sample is irradiated under UV light during around six hours. Samples from the suspension (0.3 mL) are taken at regular time intervals for analysis. They are analyzed by HPLC Varian ProStar 410 analysis using a COREGEL 87H 3 (300 mm × 7.8 mm) and a Varian Prostar 325 detector (detection at 210 nm). Injection volume is 50 mL, mobile phase is sulfuric acid (5 mM) with a flow rate of 0.7 mL/min. Each experiment is performed twice to verify the reproducibility of the results and reduce the number of samplings for analyses, which could affect the total volume and consequently the kinetics determination.

To follow the coating stability, analyses are performed in pure water following the previous protocol. Pollutants released are detected by HPLC.

The evaluation of the self-cleaning properties is achieved by monitoring the methylene blue degradation according to ISO norm

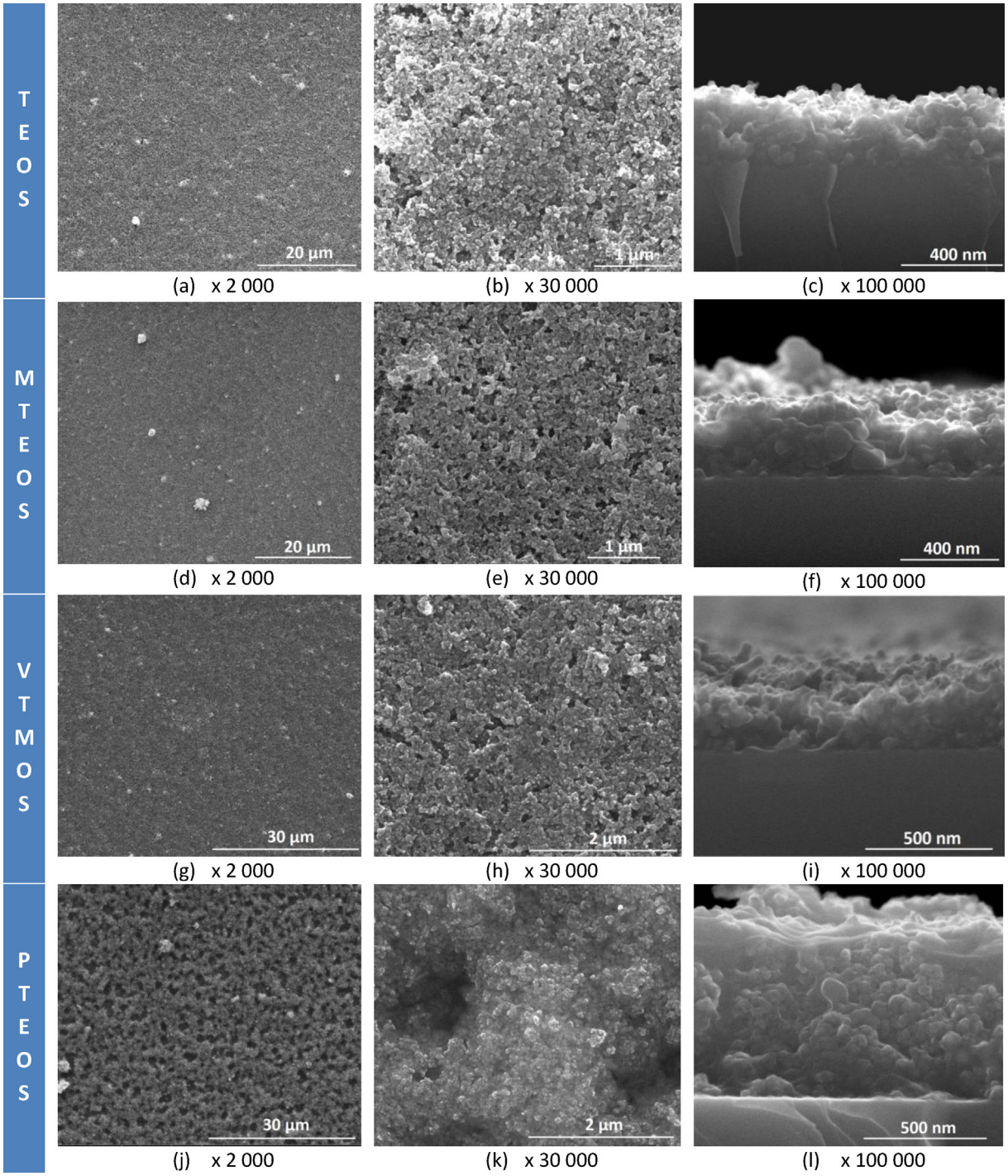

Fig. 1. SEM images of the surface and the cross-section (c, f, i and l) of coatings: pure inorganic silica coating (a–c), hybrid methyl functionalized silica coating (d–f), vinyl functionalized silica coating (g–i) and propyl functionalized silica coating (j–l).

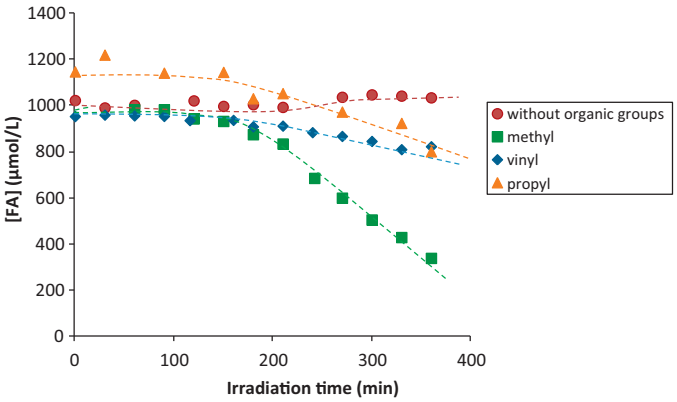

Fig. 2. FA disappearance as a function of irradiation time according to the organic group of the silica matrix.

(ISO/CD 10678). The initial concentration of the dye is 10 µmol/L. The same reactor is used with a dye volume of 35 mL. The sample is remained 30 min in obscurity before being irradiated with UVA at 365 nm (HPK 125W lamp and 0.52 filters), at a photon flux between 1 and 10 mW/cm^2. The discoloration is monitored by UV–vis spectrometer (PerkinElmer, lambda45) following the dye absorption at 664 nm. Formic acid or methylene blue degradation rates are determined with the slope curves representing the pollutant concentration according to the irradiation time.

3. Results and discussion

Composite porous films embedding TiO_2 nanoparticles into a hybrid silica matrix are prepared. The composition of the matrix depends on the starting functional alkoxysilane precursor. The general preparation method is similar to the one used in previously reported photocatalytic flexible coatings [20]. Here we propose investigation on the impact of the precursor structure on the final material and photocatalytic activity.

3.1. Structure and morphology

The presence of organic groups into the silica matrix allows bringing flexibility to the coating. For this reason, it is interesting to try to vary the size of these organic groups and check influence on the final properties. The impact of the precursor on the coating structuration is shown in Fig. 1 with the scanning electron microscopy (SEM) images of the various composite coatings. All coatings present an important porosity. This porosity is generated during the coating process without surfactant according to a previously reported mechanism [20]. Scanning electron microscopy (SEM) images clearly show the presence of homogeneouly dispersed TiO_2 particles encapsulated in a matrix gangue made of hybrid silica (Fig. 1). While most of the coatings present similar thickness, of about 300 nm (Fig. 1c,f and i), the propyl-functionalized silica coatings show larger pores with sizes between 1 and 5 µm (Fig. 1j and k) and larger thickness (680 nm, Fig. 1l). Moreover, the visual aspect of the deposited coating is more whitish. The difference in porosity is probably related to the instability of the propyl-functionalized silica sol due to a higher hydrophobicity. This latest formulation is also more sensitive to the temperature and the coating conditions.

The TiO_2 amount in the coatings is measured using inductively coupled plasma analysis (ICP) as about 0.05 mg/cm^2 in coatings obtained from TEOS, MTEOS and VTMOS-functionalized sols, and about 0.07 mg/cm^2 in the case of the propyl-functionalized silica coatings.

The incorporation of organic pending groups into the silica matrices strongly affects the coating properties and in particular hydrophobicity. The contact angle is higher in the case of coatings obtained from organic modified silica sol (120°) than for pure silica (12°). However, no influence of the functional group size is observed (data not illustrated).

3.2. Photocatalytic activity and stability of the composite coatings

3.2.1. Formic acid (FA) degradation

The photocatalytic activity is evaluated following the disappearance of formic acid as a function of the UV irradiation time. Formic acid is chosen as model since its photocatalytic decomposition

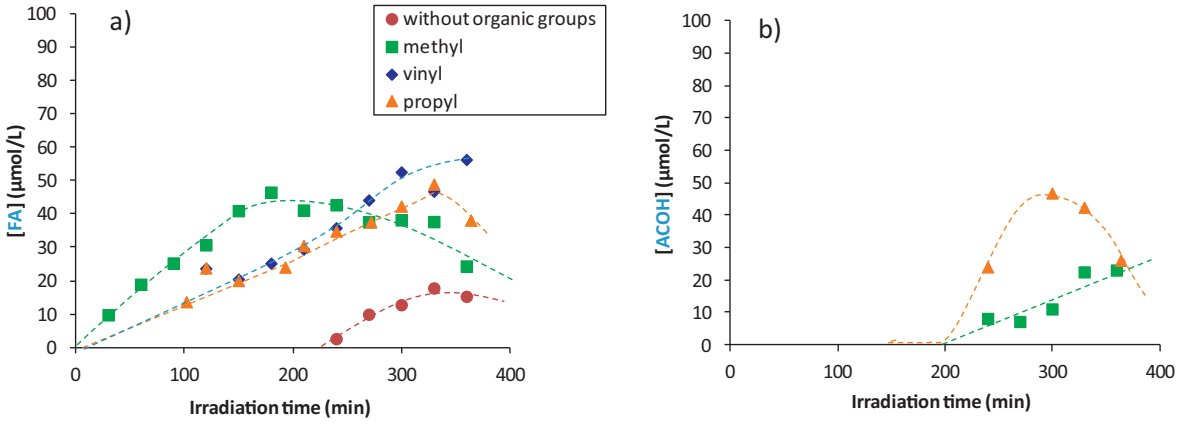

Fig. 3. (a) formic acid and (b) acetic acid release according to the silica pending organic group.

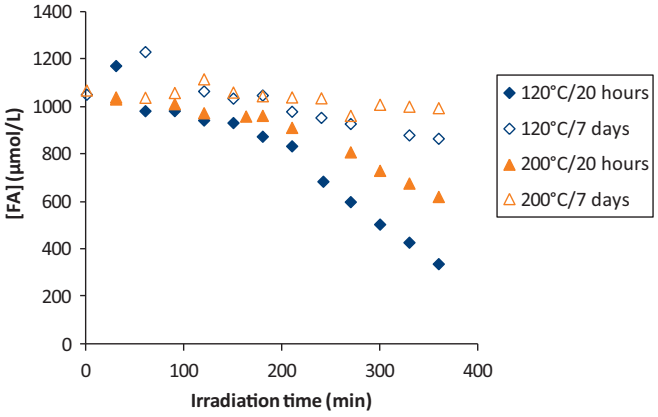

Fig. 4. Influence of the heating time and temperature of the drying step of methyl functionalized silica coating on the FA degradation.

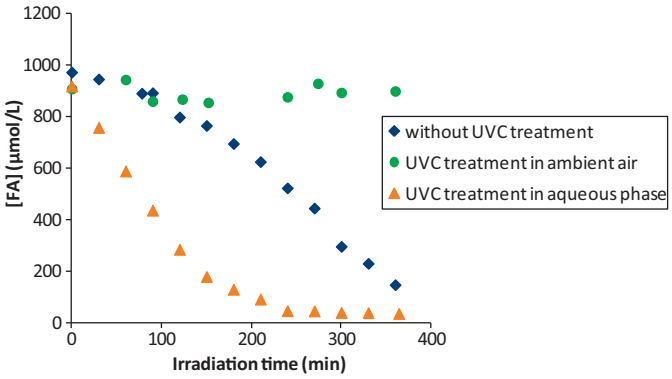

Fig. 6. Influence of the UVC pretreatment conditions (ambient air, aqueous phase) of methyl functionalized silica coating on its photocatalytic activity (FA degradation).

produces no intermediate compounds, only final CO_2 [36]. Moreover, the formic acid degradation appears to be a common last step in all the photocatalytic decomposition reactions. The results on all the prepared composites are shown in Fig. 2. We note that in all cases no formic acid decomposition is observed before 200 min of UV exposure. It can be linked to a self-cleaning step corresponding to the degradation of the hybrid silica pending organic groups which are in contact with TiO_2. After this period, the coating activity varies depending on the size of the organic pending groups in the matrices. The composites bearing methyl groups become more rapidly active. After 6 h of irradiation, around 75% of formic acid is degraded whereas less than 20% is removed for the other coatings. It is also important to highlight that coatings without silica organics groups are totally inactive. Moreover, the FA concentration seems to increase after about 200 min of irradiation suggesting that the organic molecules, scavenged into the matrix, are degraded. In order to understand the activation step, evaluation of the coating stabilization is investigated.

3.2.2. Coating stabilization

The coating stabilization step is monitored following the pollutant release in water under UV irradiation. Analyses are realized without pollutant, immersing directly the coating in water. According to the type of matrix, various organic compounds are detected by HPLC. Formic acid is the main pollutant released. Its formation occurs more rapidly with methyl groups than with vinyl and propyl groups (Fig. 3a). Moreover, FA generation is also observed for the inorganic matrix but its detection is only observed after about 220 min of irradiation. This result is in agreement with the slight increase of FA observed in Fig. 2 after 200 min. It suggests that the FA released can also be formed by the degradation of ethanol (solvent) and/or acetic acid (dispersing agent), entrapped into the matrix [37].

Acetic acid (AcOH) is also released by coatings bearing methyl and propyl groups (Fig. 3b). For propyl functionalized silica films, the presence of AcOH can result from the organic groups degradation [38,39]. In the case of methyl functionalized coatings, the formation of compounds with higher carbon ratio can occur from the recombination of the degraded organic groups [40] or from the solvent or dispersing agent. This is not observed for inorganic or vinyl based matrices during the chosen irradiation time. This result is in agreement with the mechanism proposed in the literature for the vinyl groups degradation. Actually, according to Hauchecorne et al. [41], under UV, double bonds are opened to form a diol and are broken in two molecules of formaldehyde and then formic acid. In the case of silica propyl groups, pyruvic acid is also detected during the test. Its formation confirms the degradation of the silica organic groups. Indeed, pyruvic acid is observed in the degradation of propanoic acid [42].

Thus, under UV, the coatings appear to evolve during a specific period of time prior to get stabilized. They release compounds which are specific to both the silica organic functional groups and the organic compounds remained trapped into the porous material walls. It means that the coating initially generates pollutants,

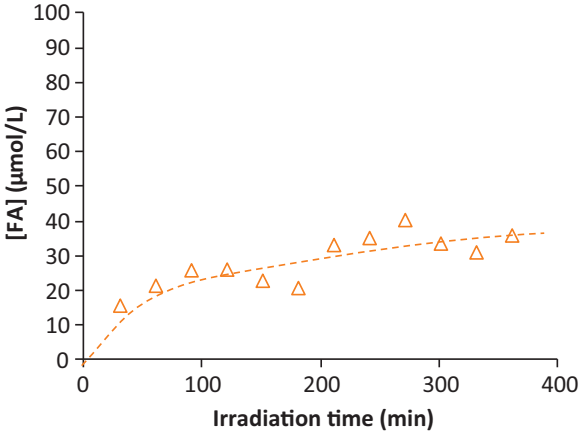

Fig. 5. Formic acid released after a thermal treatment of 7 days at 200 °C of methyl functionalized silica coating.

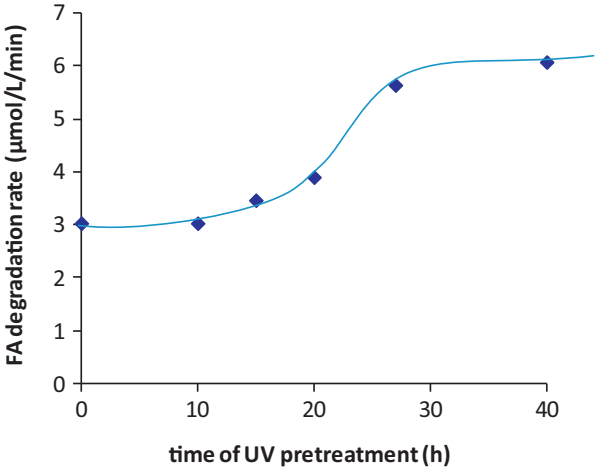

Fig. 7. Influence of the UVC irradiation time of methyl functionalized silica coating on its photocatalytic activity (FA degradation).

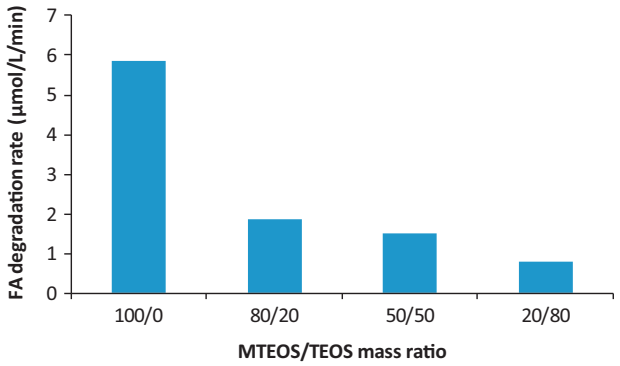

Fig. 8. Influence of MTEOS/TEOS mass ratio on the photocatalytic activity (FA degradation) of UVC pretreated coatings (27 h).

which impact the early photocatalytic activity of the coating. The longer is the pending group, the more intermediates are generated and longer time is required to clean and stabilize the composite system.

The objective being to obtain a final material active and stable, it is crucial to remove efficiently the organic groups near TiO_2 particles and the other compounds adsorbed in the coating porosity. Two different processes are reported here: thermal and UV treatments.

3.3. Impact of the treatments

Treatments are performed only on coatings prepared with MTEOS precursors which appeared to be the most interesting and efficient for our application. BET (nitrogen) analyses are performed on the hybrid silica composite and a BET surface of 210 m^2/g is obtained.

3.3.1. Thermal treatment

The thermal treatment is a common way to eliminate organics [21–23]. A sustained heat treatment is realized to remove solvents traces and avoid pollutant release by the coating. Methyl coatings are heated at 120 °C or 200 °C for 20 h or 7 days. A decrease of the photocatalytic activity is observed with the increase of the drying time and temperature (Fig. 4). Moreover, formation of FA is always observed after heating at 200 °C during 7 days (Fig. 5) which confirms that organic compounds are still present in the coating. Surface analyses confirm the conservation of the silica pending organic groups. No change in the chemical composition is observed by XPS. O—Si/Si (O—Si corresponds to the part of the O1s signal limited to O—Si chemical binding) and C—Si/Si ratios (C—Si corresponds to the part of the C1s signal limited to C—Si chemical binding) exhibit the same values of, respectively, 1.5 ± 0.06 and 1 ± 0.02 corresponding to silicon bonded to 3 oxygen atoms and 1 organic group (data not illustrated). These results confirm that organic groups remain trapped. Thermal treatment cannot be considered as efficient to improve the coating stability and activity.

3.3.2. UV treatment

The samples are irradiated under UVC at 254 nm for 27 h. The irradiations are realized in ambient air or in aqueous phase, immersing samples in pure water. The treatment of the coating in ambient air induces a total loss of activity (Fig. 6). However, when samples are immersed in water, the UV treatment allows promoting the coating activity by a factor 2. In these conditions, 90% of FA is degraded after 180 min with UV preliminary treatment against 380 min without light treatment. The coating is then directly active and does not present any "self-cleaning step". The water role can be explained in two ways: (i) it promotes the $OH^{\bullet}$ formation, highly oxidizing radicals, and/or (ii) favor the elimination of the intermediate organic compounds, remaining into the porosity. The removal of organic groups and their photodegradation products probably allow improving the accessibility to the photocatalyst, promoting the photocatalytic activity. Elimination of the silica organic pending groups is confirmed by XPS [20]. O—Si/Si ratio increased to 2 ± 0.1 after the UV irradiation corresponding to a SiO_2 structure with silicon in chemical binding with four oxygen atoms. The degradation of the organic compounds is also observed with the C—Si/Si ratio, which strongly decreases after the UV treatment from 1 ± 0.04 to 0.1 ± 0.05. The organic groups removal also induces a decrease of the contact angle (8°), which remains constant even after 1 month of storage in dark (see Fig. SI2). The UV treatment presents the advantage to target the organic groups in contact with TiO_2 and efficiently eliminate them via the photocatalytic process. Moreover, no pollutant release is observed after a UV treatment in aqueous phase. Thus, with optimized conditions, UV preliminary treatment appears to be an efficient method to obtain stable and active materials.

A second parameter investigated is the irradiation time. This factor is optimized in order to obtain the best photocatalytic efficiency. The samples are immersed in water and irradiated for 40 h under UVC. The photocatalytic efficiency increases with the irradiation time. Fig. 7 shows that an optimum of activity is reached after around 25–30 h of UV exposure. It is interesting to note that similar

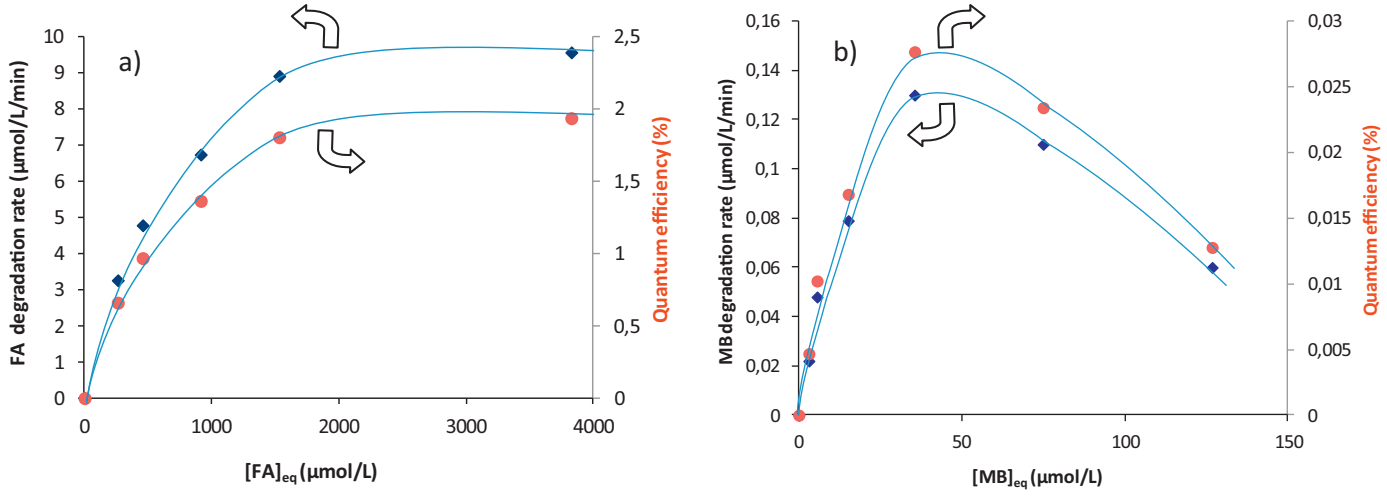

Fig. 9. Influence of the pollutant concentration on (a) formic acid and (b) methylene blue degradation rates and photonic efficiency for UVC pretreated coatings (27 h).

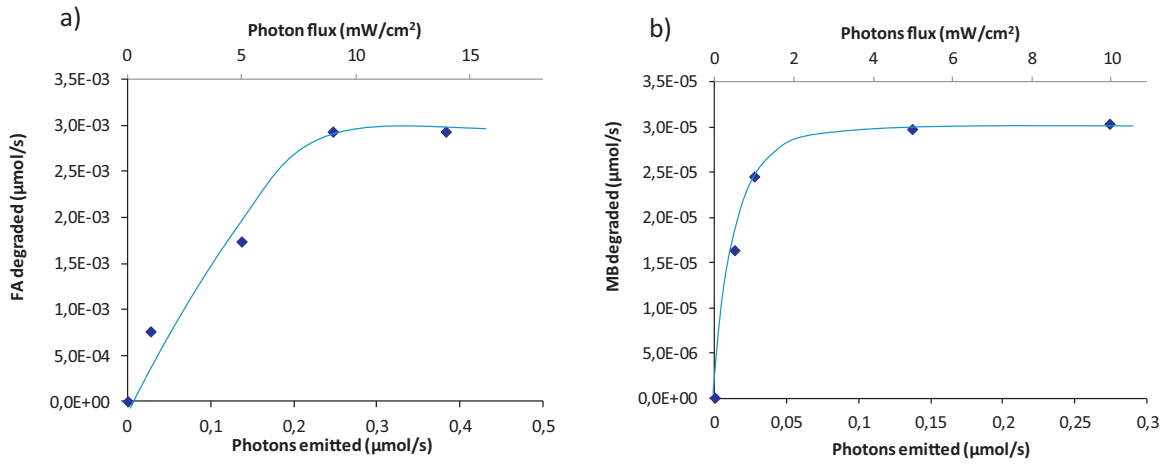

Fig. 10. Influence of the photon flux on (a) acid formic and (b) methylene blue degradation rates for UVC pretreated coatings (27 h).

efficiency is obtained under UVA (365 nm) after 27 h of irradiation. With the UV treatment, the photocatalytic efficiency remains constant even after several recycling tests.

3.4. Role of the silica organic pending groups ratio

With the idea to correlate the use of silica organic pending groups and the photocatalytic efficiency, matrices are prepared with different ratios of organic groups versus silica. Various proportions of methylated sol (from MTEOS precursor) and pure inorganic sol (from TEOS precursor) are combined. MTEOS/TEOS mass ratio is tuned while maintaining in all cases a sol with composition of 10% wt in silica and 10% wt in TiO_2. Then, the coatings are treated for 27 h under UVC. Fig. 8 shows the photocatalytic efficiency which decreases significantly while lowering the MTEOS/TEOS ratio. This result demonstrates that the incorporation of silica organic pending groups, partially eliminated by photonic treatment, is essential and contributes strongly to the final photocatalytic activity of the films.

3.5. Depolluting and self-cleaning properties of the coatings

The self-cleaning performance of the most efficient coating is evaluated using methylene blue (MB) according to ISO standard (ISO/CD 10678) [43].

3.5.1. Effect of the pollutant concentration

The pollutant adsorption at the catalyst surface is an initial and primordial step to optimize the photocatalytic reactions. Samples are placed 30 min in dark prior to be irradiated to reach the adsorption equilibrium. When FA and MB concentrations increase, the quantity of organic adsorbed by the coating increases too, before reaching a plateau corresponding to the maximal amount of pollutant adsorbed (Q_{max}) [44,45]. In our case, organic adsorption can occur on TiO_2 surface but also on the silica matrix. Indeed, Q_{max} calculated for our materials (1.6 µmol/cm^2 for FA, corresponding to 16 mmol/g of TiO_2) is important compared to Q_{max} for TiO_2 powder [44] indicating that the major part of organic compounds is adsorbed on the binder and/or trapped into pores. The same observations are made for MB. MB is also adsorbed in large quantity at the accessible surface of the film (Q_{max} = 0.02 µmol/cm^2 corresponding to 0.2 mmol/g of TiO_2).

Under UV exposure, FA and MB degradation rates increase proportionally with the initial pollutant concentration until a maximum rate (Fig. 9a and b). In the case of FA, a plateau is reached whereas, for MB, the disappearance rate decreases with the pollutant concentration (Fig. 9a and b). It can be explained by the spectral absorption related to the dyes. Increasing the dye concentration affects the light penetration into the solution and less photons are able to reach the photocatalyst surface [46]. Thus, the generation of active species $OH^{\bullet}$ and $O_2^{\bullet -}$ is less effective and impacts the efficiency of the catalytic reactions. At low concentration, for both compounds, a pseudo first apparent order kinetic rate is observed corresponding to about 0.011 min^{-1} for FA and 0.008 min^{-1} for MB. However, it is important to highlight that the disappearance of MB is determined by spectrophotometry, which means a global measurement of the discoloration and not the disappearance of molecules. Thus, intermediate compounds can also be colored and thus detected, minimizing the disappearance rate of MB.

In the case of FA, Langmuir–Hinshelwood equation can be used to model the kinetics (Eq. (1)) allowing the determination of k and K.

$$r_0 = \frac{kKC_e}{1 + KC_e}$$

With C_e : FA concentration at the equilibrium (1)

With k, the disappearance rates in mol L^{-1} min^{-1} and K the adsorption constant in L mol^{-1}. K and k are estimated to be, respectively, of 8.3×10^{-4} L µmol^{-1} and 12 µmol L^{-1} min^{-1}. In the case of MB, k and K are not determined because a decrease of disappearance rate is observed at about 35 µmol/L.

Fig. 9 shows the photonic efficiency in the right scale, defined as the number of molecules degraded per second over the number of photons emitted by the lamp per second. In the case of the use of a dye like MB, we precise that the photonic efficiency calculated associates the photocatalytic degradation and the direct photodegradation of the dye. The photonic efficiency increases as a function of the initial pollutant concentration with a slope of about 0.0022 and 0.0015% per µmol/L for, respectively, FA and MB, before reaching a plateau. Increasing the pollutant concentration induces an increase in the coverage rate of the catalyst and a decrease in the recombination of electron/hole pairs.

This shows that this type of materials can be used to remove efficiently pollutants present in water at low concentration such as pharmaceutical products or endocrine disruptor considering a first order kinetic rate. The zero order kinetic rate can be considered in the case of non-colored waste water containing high concentration of pollutants. In the case of colored wastewater at high concentration of pollutant, the more the solution is colored, the less efficient is the material.

3.5.2. Effect of the photons flux

The study of photon flux effect is relevant since the optimized coatings target applications under solar and artificial light. A maximal solar photon flux is generally observed between 4 and 5 mW/cm^2 [47,48]. The photon flux is varied between 0.5 and 14 mW/cm^2 (Fig. 10). In the dark, coatings are not active. At low concentration of photons, the disappearance rate is proportional to the photon flux. Then, a plateau is reached corresponding to the recombination of photogenerated electrons–holes [49]. The plateau is not reached at same photon flux for both organic compounds. Disappearance rate is stabilized at about 2 mW/cm^2 for MB solution and 9 mW/cm^2 for FA corresponding to a photonic efficiency of, respectively, 0.03% and 1.2%. These results can be explained by the initial concentration of MB and FA used of, respectively, 10 μmol/L and 1086 μmol/L. One can note that the photonic efficiency depends on the pollutant concentration. It means that at low concentration, less photons are necessary to degrade the pollutant. Thus, the smallest is the pollutant concentration, the lowest is the number of required photons. This result is of importance for further solar water treatment applications.

4. Conclusion

The relationship between the matrix chemical composition, and thus the structure, and the photocatalytic properties of the films is deeply investigated. Particular attention is brought to the possibility of using solar energy conditions as excitation source. Photocatalytic activity and stability of composite coatings, consisting of commercial TiO_2 nanoparticles dispersed into a hybrid silica matrix containing Si—C functional bonds, are studied using formic acid as model pollutant. We show that the structure of the coatings is evolving at the beginning of the irradiation for a limited period of time releasing organic compounds coming mostly from the silica organic pending groups. A cleaning preliminary step is then processed to obtain an active and stable photocatalytic material. Moreover, the removal of the pending organic groups is necessary to optimize the microstructure and particular porosity and open efficiently the interaction between the catalysts and the adsorbed pollutants. The use of hybrid organically modified silica matrix is thus demonstrated to be necessary to improve the pollutant accessibility to the TiO_2 active sites. These materials are also investigated in irradiation conditions comparable to solar light excitation and are clearly efficient in these conditions. As a conclusion, they can be efficiently used as self-cleaning materials and for water depollution using solar light. These materials can easily be processed on all type of substrates such as silica and even thermosensitives and flexibles ones, such as organics substrates, textiles, plastics, papers, keeping the flexibility properties.

Acknowledgements

Authors would like to thank Céline Brunon from Science et Surface for SEM and XPS spectra.

This project was funded by the French FUI call as part of the COMPHOSOL2 project, supported by Techtera, the competitiveness cluster for technical and functional textiles based in the Rhône-Alpes region (France).

Appendix A. Supplementary data

Supplementary data associated with this article can be found, in the online version, at http://dx.doi.org/10.1016/j.apcatb.2015.04.005.

References

[1] A. Machulek, S.C. Oliveira, M.E. Osugi, V.S. Ferreira, F.H. Quina, R.F. Dantas, S.L. Oliveira, G.A. Casagrande, F.J. Anaissi, V.O. Silva, R.P. Cavalcante, F. Gozzi, D.D. Ramos, A.P.P. da Rosa, A.P.F. Santos, D.C. de Castro, J.A. Nogueira, Organic pollutants-Monitoring, risk and treatment, In: M. Nageeb Rashed (Ed.), 2013, pp.141–166.
[2] C. Guillard, D. Debayle, A. Gagnaire, H. Zaffrezic, J.-M. Herrmann, Mater. Res. Bull. 39 (2004) 1445–1458.
[3] J.M. Herrmann, J. Photochem. Photobiol. A 216 (2010) 85–93.
[4] J.-M. Herrmann, Top. Catal. 34 (2005) 49–65.
[5] S. Cho, W. Choi, J. Photochem. Photobiol. A 143 (2001) 221.
[6] X.D. Chen, Z. Wang, Z.F. Liao, Y.L. Mai, M.Q. Zhang, Polym. Test. 26 (2007) 202.
[7] M. Radetic, J. Photochem. Photobiol. C 16 (2013) 62–76.
[8] D.P. Macwan, P.N. Dave, S. Chartuvedi, J. Mater. Sci. 46 (2011) 3669–3686.
[9] H. Zhang, H. Zhu, Appl. Surf. Sci. 258 (2012) 10034–10041.
[10] B. Tan, B. Gao, J. Guo, X. Guo, M. Long, Surf. Coat. Tech. 232 (2013) 26–32.
[11] S.M. Gupta, M. Tripathi, Cent. Eur. J. Chem. 10 (2) (2012) 279–294.
[12] W.A. Daoud, J.H. Xin, Y.-H. Zhang, Surf. Sci. 599 (2005) 69–75.
[13] S.R. Meher, L. Balakrishnan, Mater. Sci. Semicond. Process 26 (2014) 251–258.
[14] N. Abidi, L. Cabrales, E. Hequet, ACS Appl. Mater. Interfaces 1 (10) (2009) 2141.
[15] E. Pakdel, W.A. Daoud, J. Colloid Interface Sci. 401 (2013) 1.
[16] G. Goncalves, P.A.A.P. Marques, R.J.B. Pinto, T. Trindade, N.C. Pascoal, Compos. Sci. Technol. 69 (2009) 1051.
[17] M.I. Mejia, J.M. Marin, G. Restrepo, L.A. Rios, C. Pulgarin, J. Kiwi, Appl. Catal. B-Environ. 94 (2010) 166–172.
[18] T. Yuranova, R. Mosteo, J. Bandara, D. Laub, J. Kiwi, J. Mol. Catal. A-Chem. 244 (2006) 160.
[19] D.Y. Nadargi, S.S. Latthe, H. Hirashima, A.V. Rao, Micropor. Mesopor. Mater. 69 (2009) 1051.
[20] D. Gregori, I. Benchenaa, F. Chaput, S. Therias, J.-L. Gardette, D. Léonard, C. Guillard, S. Parola, J. Mater. Chem. A 2 (2014) 20096.
[21] H.U. Lee, S.C. Lee, J.H. Seo, W.G. Hong, H. Kim, H.J. Yun, H.J. Kim, J. Lee, Chem. Eng. J. 223 (2013) 209.
[22] J.M. Calderon-Moreno, S. Preda, L. Predoana, M. Zaharescu, M. Anastasescu, M. Nicolescu, M. Stoica, H. Stroescu, M. Gartner, O. Buiu, M. Mihaila, B. Serban, Ceram. Int. 40 (2014) 2209–2220.
[23] S. Suarez, N. Arconada, Y. Castro, J.M. Coronado, R. Portela, A. Duran, B. Sanchez, Appl. Catal. B- Environ. 108–109 (2011) 14–21.
[24] G. Buchel, R. Denoyel, P.L. Llewellyn, J. Rouquerole, J. Mater. Chem. 11 (2001) 589–593.
[25] S. Heng, P.P.S. Lau, K.L. Yeung, M. Djafer, J.-C. Schrotter, J. Membr. Sci. 243 (2004) 669–678.
[26] J. Kecht, T. Bein, Micropor. Mesopor. Mater. 116 (2008) 123–130.
[27] L. Xiao, J. Li, H. Jin, R. Xu, Micropor. Mesopor. Mater. 96 (2006) 413–418.
[28] A.N. Parikh, A. Navrotsky, Q. Li, C.K. Yee, M.L. Amweg, A. Corma, Micropor. Mesopor. Mater. 76 (2004) 17–22.
[29] S. Chu, L. Luo, J. Yang, F. Kong, S. Luo, Y. Wang, Z. Zou, Appl. Surf. Sci. 258 (2012) 9664–9667.
[30] M. El Roz, L. Lakiss, V. Valtchev, S. Mintova, F. Thibault-Starzyk, Micropor. Mesopor. Mater. 158 (2012) 148–154.
[31] Q. Guo, P. With, Y. Liu, R. Glaser, C.-J. Liu, Catal. Today 211 (2013) 156–161.
[32] Y. Liu, Y. Pan, Z.-J. Wang, P. Kuai, C.-J. Liu, Catal. Commun. 11 (2010) 551–554.
[33] S. Rtimi, C. Pulgarin, R. Sanjines, J. Kiwi, Appl. Catal. B 162 (2015) 236–244.
[34] D. Gregori, C. Guillard, F. Chaput, S. Parola, J. Mater. Chem. A 2 (2014) 20096–20104.
[35] D. Chateau, F. Chaput, C. Lopes, M. Lindgren, C. Brännlund, J. Öhgren, N. Djourelov, P. Nedelec, C. Desroches, B. Eliasson, T. Kindahl, F. Lerouge, C. Andraud, S. Parola, ACS Appl. Mater. Interfaces 4 (2012) 2369.
[36] M.F.J. Dijkstra, H.J. Panneman, J.G.M. Winkelman, J.J. Kelly, A.A.C.M. Beenakers, Chem. Eng. Sci. 57 (2002) 4895–4907.
[37] T. Muggli, J. McCue, J. Falconer, J. Catal. 173 (1998) 470–483.
[38] D. Vildozo, R. Portela, C. Ferronato, J.-M. Chovelon, Appl. Catal. B-Environ. 107 (2011) 347–354.
[39] C. Guillard, J. Photochem. Photobiol. A 135 (2000) 65–75.
[40] G.L. Chiarello, M.H. Aguirre, E. Selli, J. Catal. 273 (2010) 182–190.
[41] B. Hauchecorne, T. Tytgat, S.W. Verbruggen, D. Hauchecorne, D. Terrens, M. Smits, K. Vinken, S. Lenaerts, Appl. Catal. B-Environ. 105 (2011) 111–116.
[42] Y. Ogata, K. Tomizawa, K. Takagi, Can. J. Chem. 59 (1981) 14–18.
[43] http://www.iso.org/
[44] A. Turki, C. Guillard, F. Dappozze, G. Berhault, Z. Ksibi, H. Kochkar, J. Photochem. Photobiol. A 279 (2014) 8–16.
[45] H. Lachheb, E. Puzenat, A. Houas, M. Ksibi, E. Elaloui, C. Guillard, J.-M. Herrmann, Appl. Catal. B-Environ. 39 (2002) 75–90.
[46] K. Sahel, N. Perol, H. Chermette, C. Bordes, Z. Derriche, C. Guillard, Appl. Catal. B-Environ. 77 (2007) 100–109.
[47] L.C. Navntoft, P. Fernandez-Ibanez, F. Garreta, Sol. Energy 86 (2012) 307–318.
[48] C. Guillard, J. Disdier, C. Monnet, J. Dussaud, S. Malato, J. Blanco, M. Maldonado, J.-M. Herrmann, Appl. Catal. B-Environ. 46 (2003) 319–332.
[49] J.-M. Herrmann, Top. Catal. 34 (2005) 49–65.